

Topological stability of the hippocampal spatial map and synaptic transience

Yuri Dabaghian

*Department of Neurology
The University of Texas at Houston,
McGovern Medical School, Houston, TX 77030,
*e-mail: Yuri.A.Dabaghian@uth.tmc.edu
(Dated: February 15, 2022)*

Spatial awareness in mammals is based on internalized representations of the environment—cognitive maps—encoded by networks of spiking neurons. Although behavioral studies suggest that these maps can remain stable for long periods, it is also well-known that the underlying networks of synaptic connections constantly change their architecture due to various forms of neuronal plasticity. This raises a principal question: how can a dynamic network encode a stable map of space? In the following, we discuss some recent results obtained in this direction using an algebro-topological modeling approach, which demonstrate that emergence of stable cognitive maps produced by networks with transient architectures is not only possible, but may be a generic phenomenon.

I. INTRODUCTION

General background. Spatial awareness in mammals is based on an internalized representation of the environment. Many parts of the brain are contributing to this representation, providing different types of information: cue positions [1], geometry of the navigated paths [2], orientations [3, 4], traveled distances [5, 6], velocities [7], qualitative geometric relationships [8, 9], etc. A principal question addressed by neuroscience is how all these types of data are captured by neuronal activity and what are the computational algorithms employed by various networks for processing this information.

At the current stage, our understanding of the mechanisms of spatial cognition is based mostly on empirical observations. For example, it was found that a major role in cognitive representation of the ambient space is played by the hippocampus: a vast number of experiments demonstrate that the hippocampal network contributes a “cognitive map” C that is crucial for the animal’s ability to navigate, to find its nest and food sources, etc. [10, 11]. Experimentally, the properties of the cognitive map are studied by mapping hippocampal activity into the studied environment \mathcal{E} ,

$$f : C \rightarrow \mathcal{E}.$$

In experiments with rodents (e.g., rats or mice), this mapping is constructed by ascribing the $(x - y)$ coordinates to every spike produced by the hippocampal principal neurons according to the animal’s position at the time when the spike was fired [12]. As shown in [13], such mapping produces spatial clusters of spikes, indicating that these neurons, known as the “place cells,” fire only in certain places—their respective “place fields.” The spatial layout of the place fields in \mathcal{E} —the place field map $M_{\mathcal{E}}$ (Fig. 1A)—is therefore viewed as a geometric representation of the cognitive map of that particular environment, $C(\mathcal{E})$. Electrophysiological recordings in “morphing” arenas demonstrate that $M_{\mathcal{E}}$ is flexible: as the environment is slowly deformed, the place fields shift and change their shapes, but largely preserve their mutual overlaps, adjacency and containment relationships [14–17]. Thus, the order in which the place cells spike during the animal’s navigation remains invariant within a certain range of geometric transformations [18–23], which implies that $C(\mathcal{E})$ may be viewed as a coarse framework of qualitative spatiotemporal relationships rather than precise geometry, i.e., that the hippocampal map is topological in nature.

From the computational perspective, this observation suggests that the information contained in place cell spiking should be interpreted topologically. In [24–29] we proposed an approach for such analyses, based on a schematic representations of the information supplied by place cells (co)activity. Specifically, if groups of coactive place cells, e.g., c_0, c_1, \dots, c_n , are viewed as abstract simplexes, $\sigma = [c_0, c_1, \dots, c_n]$, then the pool of the coactive place cell combinations observed by a given moment t forms a simplicial “coactivity complex” $\mathcal{T}(t)$ whose topology represents the topological structure of the cognitive map of the underlying environment (see [24–29] and Fig. 1B).

The evolution of $\mathcal{T}(t)$ reflects how the net spatial information accumulates in time: starting from a few simplexes at the beginning of navigation, the complex $\mathcal{T}(t)$ grows and eventually, if the parameters of spiking activity fall within the biological range of values, assumes a shape that is topologically equivalent to the shape of the navigated environment in a biologically plausible period T_{\min} —a theoretical estimate of the time required to “learn” the environment [24–29].

Curiously, the key building blocks of this model—the coactive groups of the hippocampal place cells represented by the coactivity simplexes, have physiological counterparts, called “cell assemblies”—functionally interconnected groups of neurons that work as operational units of the hippocampal network [30, 31]. In [32] it was shown that this correspondence can be made accurate: the construction of the coactivity complex may be adjusted so that its maximal simplexes

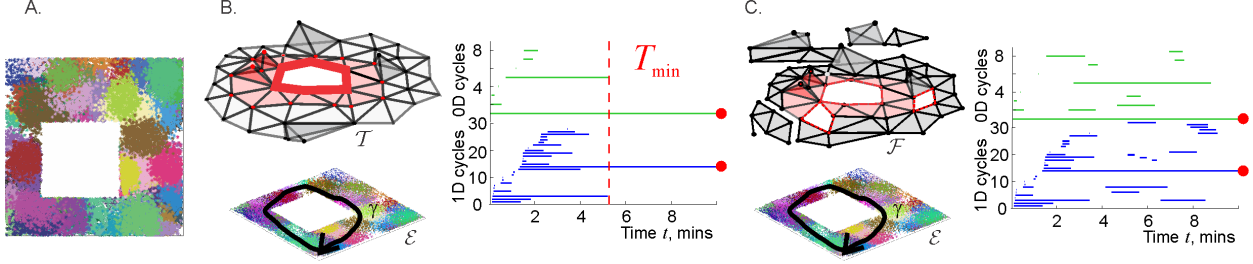


FIG. 1: Place cells and cell assemblies. (A). Simulated place field map $M_{\mathcal{E}}$ in a small ($1m \times 1m$) planar environment \mathcal{E} with a square hole: dots of a particular color, marking the locations where a specific place cells produced spikes, form spatial clusters—the place fields. Shown is a map produced for $N = 300$ place cells with a median maximal firing rate $f = 14$ Hz and place field size 20 cm. (B). The net pool of coactivities is represented by the coactivity complex \mathcal{T} (top), which provides a topological representation of the environment \mathcal{E} (bottom). E.g., the non-contractible simplicial path shown by red chain of simplexes corresponds to a non-contractible physical path γ around the central hole in \mathcal{E} . The coactivity complex \mathcal{T} assumes its topological shape as the spatial information provided by the place cells accumulates. The panel on the right shows the timelines of 0D (top) and 1D (bottom) topological loops in \mathcal{T} , computed using Persistent Homology theory methods [49–52]. The minimal time T_{\min} required to eliminate the spurious loops and extract the persistent ones (marked by the red bullets) provides an estimate for the time required by a given place cell ensemble to learn the topological structure of the navigated environment [24–29]. (C). If the simplexes may not only appear but also disappear, then the structure of the resulting “flickering” coactivity complex $\mathcal{F}(M_{\mathcal{E}})$ may never saturate, i.e., transient topological defects, described by Zigzag Persistent Homology theory [53–55] may persist indefinitely.

(i.e., the simplexes that are not subsimplexes of any larger simplex) represent place cell assemblies, rather than arbitrary combinations of coactive place cells. An important physiological property of the cell assemblies is that these are *dynamic* structures: they may form among the cells that demonstrate repeated coactivity and disband as a result of deterioration of synaptic connections, caused by reduction or cessation of spiking, then reappear due to a subsequent surge of coactivity, then disband again and so forth [30, 31]. In the model, the appearance and disappearance of the cell assemblies is represented by the appearances and disappearances of the corresponding simplexes, so that the rewiring dynamics of the cell assembly network and the dynamics of the resulting cognitive map is represented by a dynamic—“flickering”—cell assembly complex, denoted below as $\mathcal{F}(t)$. Unlike its “perennial” counterpart $\mathcal{T}(t)$ that can only grow and stabilize with time, the flickering complex $\mathcal{F}(t)$ may inflate, shrink, fragment into pieces, produce transient holes, fractures, gaps and other dynamic “topological defects” (Fig. 1C).

Thus, on the one hand, the dynamics of $\mathcal{F}(t)$ may be viewed as a natural consequence of the network’s plasticity: studies show that the lifetime of the hippocampal cell assemblies ranges between minutes [33–35] and hundreds of milliseconds [36, 37], suggesting that the hippocampal network perpetually rewires [38]. On the other hand, behavioral and cognitive studies show that spatial memories in rats can last for days and months [39–41]. This poses a principal question: *how can a large-scale spatial representation of the environment be stable if the neuronal substrate changes at a much shorter timescale?*

A principal answer to this question is suggested by an algebro-topological model of the dynamic cell assembly networks, which allows studying the effect produced by the synaptic transience on the large-scale representation of space and demonstrating that a stable topological map can form within a biologically plausible period, similar to the “perennial” learning period $T_{\min}(\mathcal{T})$, despite the rapid transience of the connections [42–45].

The large-scale topology of the cognitive map $C(\mathcal{E})$, as represented by a coactivity complex, can be described at different levels. A particularly concise description of a topological shape is given in terms of its topological loops (non-contractible surfaces identified up to topological equivalence) in different dimensions, i.e., by its Betti numbers b_n , $n = 0, 1, \dots$ [46, 47]. For example, the number of inequivalent topological loops that can be contracted to a zero-dimensional (0D) vertex, $b_0(\mathcal{F})$, corresponds to the number of the connected components in $\mathcal{F}(t)$; the number of loops that contract to a one-dimensional (1D) chain of links, $b_1(\mathcal{F})$, defines the number of holes and so forth [46, 47]. The full list of the Betti numbers of a space or a complex X is known as its topological barcode, $\mathbf{b}(X) = (b_0(X), b_1(X), b_2(X), \dots)$, which captures the topological identity of X [48]. For example, the barcode $\mathbf{b} = (1, 1, 0, \dots)$ corresponds to a topological annulus, the barcode $\mathbf{b} = (1, 0, 1, 0, \dots)$ —to a two-dimensional (2D) sphere S^2 , the barcode $\mathbf{b} = (1, 2, 1, 0, \dots)$ —to a torus T^2 and so forth [49]. Thus, by comparing the barcode of the coactivity complex $\mathbf{b}(\mathcal{F})$ to the barcode of the environment $\mathbf{b}(\mathcal{E})$ one can establish whether their topological shapes match, $\mathbf{b}(\mathcal{F}(t)) = \mathbf{b}(\mathcal{E})$, i.e., whether the coactivity complex provides a faithful representation of the environment at a given moment t . The mathematical methods required for these analyses—Persistent Homology [49–52] and Zigzag Persistent Homology theories [53–55], also outlined in [56, 57], allow building a dynamical model of the cognitive map and addressing the question “*How can a rapidly rewiring network produce and sustain a stable cognitive map?*”

II. OVERVIEW OF THE RESULTS

An efficient implementation of the coactivity complex $\mathcal{F}(t)$ is based on the “cognitive graph” model of the hippocampal network [12, 59], in which each active place cell c_i corresponds to a vertex v_i of a graph \mathcal{G} , whose connections $\varsigma_{ij} = [v_i, v_j]$ represent pairs of coactive cells. An assembly of place cells c_0, c_1, \dots, c_n then corresponds to the fully interconnected subgraph, i.e., to a maximal clique $\varsigma = [v_0, v_1, \dots, v_n]$ of \mathcal{G} [29, 30, 32]. Since cliques, as combinatorial objects, can be viewed as simplexes spanned by the same sets of vertexes, the collection of \mathcal{G} -cliques defines a clique simplicial complex [60] that serves as an instantiation of the coactivity complex [26–29, 32]. The dynamics of the clique coactivity complexes can be modeled based on the dynamics of the links of the corresponding coactivity graph \mathcal{G} . In the following, we discuss two such approaches, both of which demonstrate a possibility of encoding stable cognitive maps by transient cell assembly networks.

A. Decaying clique complexes

Consider the following dynamics of the coactivity graph \mathcal{G} .

- The vertexes of \mathcal{G} appear when the corresponding cells become active for the first time and never disappear, since according to the experiments, place cells’ spiking in learned environments remains stable [62].
- The connection ς_{ij} between the vertexes v_i and v_j appears with probability $p_+ = 1$ if the cells c_i and c_j become active within a $w = 1/4$ second period (for biological motivations of the w -value see [25, 61]). The exact time t of the link’s appearance can be associated with any moment within w .

- An existing link ς_{ij} between cells c_i and c_j disappears with the probability

$$p_{-}(t) = \frac{1}{\tau} e^{-t/\tau}, \quad (1)$$

where the time t is counted from the moment of the link's last activation and τ defines the link's *proper* decay time.

- The dynamics of the higher order cliques, e.g., their decay times, is fully determined by the link decay period τ . In the following, the notations \mathcal{G}_τ and \mathcal{F}_τ will refer, respectively, to the flickering coactivity graph and the corresponding flickering clique coactivity complex with the connections' proper decay rate $1/\tau$.

Note that the ongoing place cell activity can reinstate some decayed links in \mathcal{G}_τ and rejuvenate (i.e., reset the decay of) some existent ones, thus producing an *effective* link's mean lifetime $\tau_e > \tau$ and leading to diverse topological dynamics of the coactivity complex \mathcal{F}_τ . As mentioned previously, a key determinant of this dynamics is the sequence in which the rat traverses place fields in a map $M_\mathcal{E}$. Fixing $M_\mathcal{E}$ and the animal's trajectory $\gamma(t)$ settles the times at which place cell combinations become active (notwithstanding the stochasticity of neuronal firing [63, 64]), so that the Betti numbers b_k of $\mathcal{F}_\tau(t)$ become dependent primarily on the parameters of neuronal spiking activity: firing rates, place field sizes, etc., and on the links' decay time τ . In the following, we will review some of these dependencies for the case of the environment shown on Fig. 1A, and discuss how they affect the net topological structure of the corresponding cognitive map. For more details see [42–45].

Dynamics of the decaying flickering coactivity complexes. If τ is too small (e.g., if the coactivity simplexes tend to disappear between two consecutive co-activations of the corresponding cells), then the flickering complex should rapidly deteriorate without assuming the required topological shape. In contrast, if τ is too large, then the effect of the decaying connections should be small, i.e., the flickering complex $\mathcal{F}_\tau(t)$ should follow the dynamics of its “perennial” counterpart $\mathcal{T}(t) \equiv \mathcal{F}_\infty(t)$, computed for the same place cell spiking parameters. In particular, if the firing rates and the place field sizes are such that $\mathcal{T}(t)$ assumes the correct topological shape in a biologically viable time $T_{\min}(\mathcal{T})$, then a similar behavior should be expected from its slowly decomposing counterpart $\mathcal{F}_\tau(t)$. However, for intermediate values of τ that exceed the characteristic interval Δt between two consecutive activations of a typical link in \mathcal{G} —a the natural timescale defined by the statistics of the rat's movements—the topological dynamics of $\mathcal{F}_\tau(t)$ may exhibit a rich variety of behaviors.

Simulations show that the characteristic inter-activation interval in the environment shown on Fig. 1A is about $\Delta t \approx 30$ seconds. For the proper decay times that generously exceed Δt , e.g., $2.5\Delta t \lesssim \tau \lesssim 4.5\Delta t$, the histogram of the time intervals $\Delta t_{\varsigma,i}$ between the i^{th} consecutive birth and death of a link ς is bimodal: the relatively short lifetimes are exponentially distributed, with the *effective* link lifetimes about twice higher $\tau_e^{(2)} \approx 2\tau$ (higher order simplexes decay more rapidly, e.g., $\tau_e^{(3)} \approx \tau$, etc.). In addition, there emerges a pool of long-living connections that persist throughout the entire navigation period (Fig. 2A). In other words, the flickering coactivity complex $\mathcal{F}_\tau(t)$ acquires a stable “core” formed by a population of “surviving simplexes,” enveloped by a population of rapidly recycling, “fluttering,” simplexes.

The numbers of d -dimensional simplexes in $\mathcal{F}_\tau(t)$ (its f -numbers in terminology of [65]) rapidly grow at the onset of the navigation, when $\mathcal{F}_\tau(t)$ inflates, but then begin to saturate by the time a typical link makes an appearance (in the case of the environment shown on Fig. 1A, this takes a few minutes). The characteristic size of $\mathcal{F}_\tau(t)$ grows to about a half of the size of its perennial

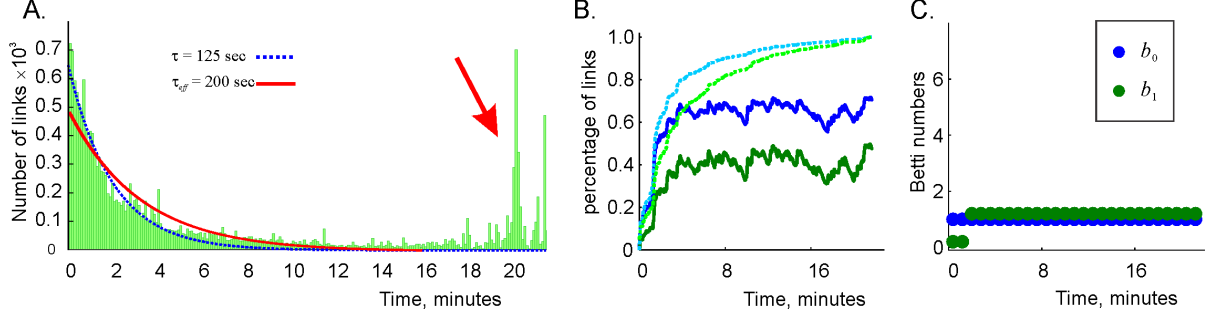


FIG. 2: **Topological dynamics of the decaying coactivity complex.** **A:** The histogram of the connections' durations between their consecutive appearances and disappearances: the shorter lifetimes are distributed exponentially (the red line fit) and the population of the “survivor” links produces a bulging tail of the distribution (red arrow). The dashed blue line shows the shape of the distribution (1). **B:** The population of 1D (blue trace) and 2D (green trace) simplexes in the decaying “flickering” complex $\mathcal{F}_\tau(t)$, compared to the population of 1D and 2D simplexes in the perennial complex $\mathcal{T}(t)$ (dashed lines). The size of $\mathcal{F}_\tau(t)$ remains dynamic, whereas $\mathcal{T}(t)$ saturates in about 10 minutes. **C:** Betti numbers $b_0(\mathcal{F}_\tau(t))$ (blue) and $b_1(\mathcal{F}_\tau(t))$ (green) remain unchanged after a short initial stabilization period.

counterpart, $\mathcal{F}_\infty(t) \equiv \mathcal{T}(t)$, with about 15% fluctuations (Fig. 2B). Thus, the population of simplexes in $\mathcal{F}_\tau(t)$ is transient: although the change of the size of $\mathcal{F}_\tau(t)$ from one moment of time to the next are relatively small, the number of simplexes that are present at a given moment of time t , but missing at a later moment t' , rapidly grows as a function of temporal separation $|t - t'|$, becoming comparable to the sizes of either $\mathcal{F}_\tau(t)$ or $\mathcal{F}_\tau(t')$ in approximately one effective link-decay span [44, 45].

Meanwhile, the large-scale topology of $\mathcal{F}_\tau(t)$ changes significantly slower: after a brief initial stabilization period that roughly corresponds to the perennial learning time $T_{\min}(\mathcal{T})$, the topological barcode $b(\mathcal{F}_\tau)$ remains similar to the barcode of the navigated environment \mathcal{E} , exhibiting occasional topological fluctuations at the T_{\min} -timescale (Fig. 2C). Thus, the coactivity complex \mathcal{F}_τ can preserve not only its approximate size, but also its topological shape, despite the ongoing recycling of its simplexes.

As τ reduces, the topological fluctuations intensify (Fig. 3) and vice versa, as τ grows, the effective lifetimes $\tau_e^{(2)}$ and $\tau_e^{(3)}$, as well as the number of the simplexes actualized at a given moment increase approximately linearly, resulting in a growing “stable core” that stabilizes the overall topological structure of $\mathcal{F}_\tau(t)$. Given the physiological range of parameters (simulated rat speed, place cell firing rates, place field sizes, etc.), a *complete suppression* of topological fluctuations in the coactivity complex is achieved after the decay times exceed a finite threshold τ_p^* , comparable to the time required to revisit a typical spot in the environment. This value gives a theoretical estimate for the rate of physiological transience that permits stable representations of the environment \mathcal{E} [44].

Alternative lifetime statistics may strongly influence the topological dynamics of the cognitive map. For example, if the links' lifetimes are fixed, i.e., if the decay probability is defined by

$$p_-(t) = \begin{cases} 1 & \text{if } t = \tau \\ 0 & \text{if } t \neq \tau, \end{cases} \quad (2)$$

then the topological structure of the resulting “quenched-decay” coactivity complex $\mathcal{F}_\tau^*(t)$ changes dramatically. Even though the rejuvenation effects widen the effective distribution of the links' lifetimes (as before, in addition to a population of short-lived links with lifetimes close to τ , there

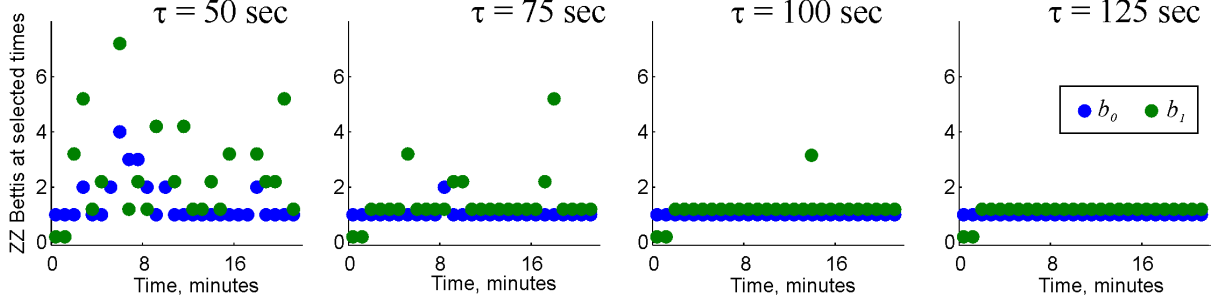


FIG. 3: **Topological stabilization.** As the decay constant τ grows, the topological shape of $\mathcal{F}_\tau(t)$ stabilizes. Shown are the Betti numbers b_0 (blue dots) and b_1 (green dots) at select moments of time, computed for several values of τ .

appears a population of the “survivor” simplexes), the resulting topological dynamics is more unstable: $\mathcal{F}_\tau^*(t)$ may split into dozens of islets containing short-lived, spurious topological defects, even for the values of τ that reliably produce physical Betti numbers for the exponentially distributed lifetimes (1).

As the decay slows down (i.e., as τ grows), the population of survivor links also grows and the topological structure of $\mathcal{F}_\tau^*(t)$ stabilizes; nevertheless, the robust, “physical” Betti numbers are attained at much (twice or more) higher values of τ than with the exponentially decaying links. Physiologically, this implies that the statistical spread of the connections’ lifetimes (the tail of the exponential distribution (1)) plays an important role: without a certain “synaptic disorder” the network is less capable of capturing the topology of the environment.

On the other hand, the topological behavior of $\mathcal{F}_\tau(t)$ is less sensitive to the *mechanism* that implements a given simplex-recycling statistics. As it turns out, even if the functional connections between place cells are established and pruned *randomly*, at a rate that matches the statistics (1), the resulting random connectivity graph $\mathcal{G}_r(t)$ produces a random clique complex $\mathcal{F}_r(t)$ with topological properties similar to those of $\mathcal{F}_\tau(t)$. In particular, the Betti numbers of $\mathcal{F}_r(t)$ converge to the Betti numbers of the environment about as quickly as the Betti numbers of its decaying counterpart $\mathcal{F}_\tau(t)$, exhibiting similar pattern of the topological fluctuations. Thus, the model suggests that the dynamic topology of the flickering complex may be controlled by the statistics of the decays and by the sheer number of simplexes present at a given moment, rather than by nature of the network’s activity (e.g., random vs. driven by the animal’s moves).

B. Finite latency complexes

An alternative model of flickering clique complexes can be built by restricting the period over which the coactivity graph is formed to a shorter time window ϖ [32]. In such approach, the coactivity simplexes that emerge within the starting ϖ -period, ϖ_1 , will constitute a coactivity complex $\mathcal{F}(\varpi_1)$; the simplexes appearing within the next window, ϖ_2 , obtained by shifting ϖ_1 over a small step $\Delta\varpi$, will form the complex $\mathcal{F}(\varpi_2)$ and so forth. For large consecutive window overlaps ($\Delta\varpi \ll \varpi$), a given clique-simplex ς (as defined by the set of its vertexes) may appear through a chain of consecutive windows, $\varpi_1, \varpi_2, \dots, \varpi_{k-1}$, then disappear at the k^{th} step ϖ_k (i.e., $\varsigma \in \mathcal{F}(\varpi_{k-1})$, but $\varsigma \notin \mathcal{F}(\varpi_k)$), then reappear in a later window $\varpi_{l \geq k}$, then disappear again, and so forth. One may then use the midpoints t_k of the windows in which ς has (re)appeared (or any other point within ϖ_k) to define the moments of ς ’s (re)births, and the matching points in the windows where it disappears to define the times of its deaths. By construction, the duration of ς ’s existence between its k -th consecutive appearance and disappearance, $\delta t_{\varsigma,k}$, can be as short as the shift step

$\Delta\varpi$ or as long as the animal's navigation session.

Simulations show that for ϖ exceeding the perennial learning time $T_{\min}(\mathcal{T})$ and $\Delta\varpi \approx 0.01\varpi$, the intervals $\delta t_{\zeta,k}$ (as well as their means averaged over k , $t_{\zeta} = \langle \delta t_{\zeta,k} \rangle_k$ and of their net existence times $\Delta T_{\zeta} = \sum_k \delta t_{\zeta,k}$) are exponentially distributed, which allows characterizing the simulated cell assemblies by a half-life, τ_{ϖ} . Specifically, for the physiological range of parameters of the neuronal activity in the environment shown on Fig. 1 and $\varpi \approx 1.2T_{\min}(\mathcal{T})$, the lifetime of a typical maximal simplex varies within $\tau_{\zeta} \approx 3 - 12$ seconds (depending on the simplex' dimensionality), which is much shorter than the proper decay time in the previous model (1) and closer to the experimentally established range of values [30].

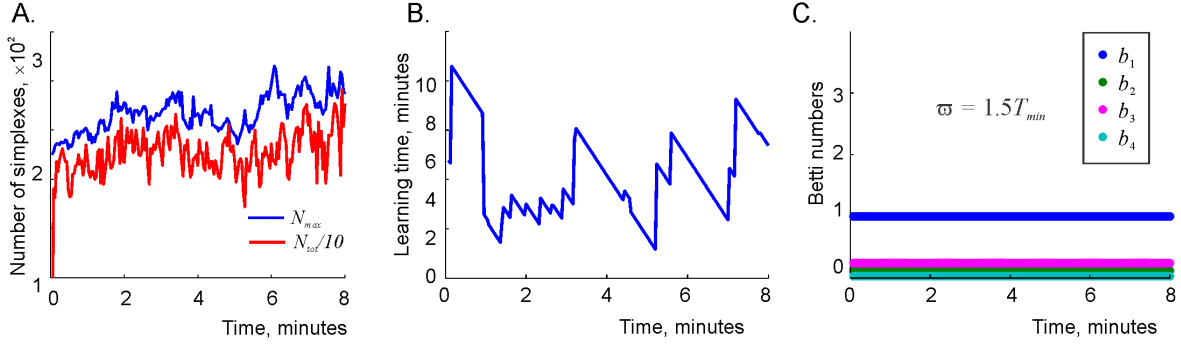


FIG. 4: **Topological dynamics in the finite latency flickering complexes.** **A.** The number of maximal simplexes (N_{\max} , blue trace) and total number of simplexes ($N_{\text{tot}}/10$, red trace) in the coactivity complex $\mathcal{F}_{\varpi}(t)$. **B.** The instantaneous learning time $T_{\min}^{(k)}$ as a function of the discrete time t_k , computed for $\varpi = 1.5T_{\min}(\mathcal{T})$. **C.** The low-dimensional Betti numbers, b_1 , b_2 , b_3 and b_4 as a function of the discrete time, computed using $\varpi = 1.5T_{\min}(\mathcal{T})$ remain stable, demonstrating full topological stabilization of $\mathcal{F}_{\varpi}(t)$.

Dynamics of the finite latency flickering coactivity complexes. It is natural to view the individual, “instantaneous” complexes $\mathcal{F}(\varpi_i)$ as instantiations of a single “finite latency” flickering coactivity complex, $\mathcal{F}(\varpi_i) = \mathcal{F}_{\varpi}(t_i)$. As it turns out, such complexes exhibit a number similarities with the decaying complexes $\mathcal{F}_{\tau}(t)$. For example, the complex $\mathcal{F}_{\varpi}(t)$ does not fluctuate significantly: for $\varpi \geq T_{\min}(\mathcal{T})$, the number of simplexes contained in $\mathcal{F}_{\varpi}(t)$ changes within about 5 – 10% of its mean value during the entire navigation period, but the pool of the *actualized* maximal simplexes is renewed at about ϖ timescale (Fig. 4A). Biologically, this implies that the simulated cell assembly network fully rewires over a ϖ period, similar to the effective link decay time $\tau_e^{(2)}$ computed in the previous model.

On the other hand, the large-scale topological properties of $\mathcal{F}_{\varpi}(t)$ are much more stable, similarly to the topological properties of $\mathcal{F}_{\tau}(t)$. For example, for sufficiently long latencies, $\varpi \gtrsim 1.2T_{\min}(\mathcal{T})$, the time required to produce the correct barcode $\mathbf{b}(\mathcal{F}_{\varpi}) = \mathbf{b}(\mathcal{E})$ within each window ϖ_k is typically finite, $T_{\min}^{(k)} = T_{\min}(\mathcal{F}(\varpi_k)) < \infty$ (Fig. 4B). Moreover, the average learning period $\bar{T}_{\min} = \langle T_{\min}^{(k)} \rangle_k$ is typically similar to the perennial learning time $T_{\min}(\mathcal{T})$, with a variance of about 20 – 40% of the mean. This result shows that the topological dynamics in the cognitive map of a semi-randomly foraging animal is largely time-invariant, i.e., the accumulation of the topological information can start at any point (e.g., at the onset of the navigation) and produce the result in an approximately the same time period. In effect, this justifies using perennial coactivity complexes for estimating T_{\min} in [24–29]. It should also be mentioned however, that there also exists a number of differences between the topological dynamics of $\mathcal{F}_{\varpi}(t)$ and $\mathcal{F}_{\tau}(t)$, e.g., the topological fluctuations in $\mathcal{F}_{\varpi}(t)$ are mostly limited to 1D loops, 2D surfaces and 3D bubbles ($b_0(t) = 1$, $b_{n>4}(t) = 0$), whereas the fluctuations in $\mathcal{F}_{\tau}(t)$ also affect higher dimensions.

As ϖ widens, the mean lifetime t_ζ of maximal simplexes grows, suppressing the topological fluctuations in $\mathcal{F}_\varpi(t)$ and vice versa, as the memory window shrinks, the fluctuations of the topological loops intensify. The proportion of the “successful” coactivity integration windows (i.e., ϖ_k s in which the correct barcode $b(\mathcal{F}_\varpi(t)) = b(\mathcal{E})$ is attained) also increases with growing ϖ . In fact, for $\varpi \geq \varpi_* \approx 1.5T_{\min}$ the topological fluctuations tend to *disappear completely* (Fig. 4C)—even though the simplexes’ lifetimes remain short ($\tau_\varpi^* \approx 15$ secs for the environment illustrated on Fig. 1A).

Moreover, it can be demonstrated that as ϖ exceeds a certain critical value ϖ_c (typically exceeding $T_{\min}(\mathcal{T})$ by less than 40%), the instantaneous learning times $T_{\min}^{(k)}$ become ϖ -independent. Thus, the finite latency model provides a *parameter-free* characterization of the time required by a network of place cell assemblies to represent the topology of the environment and establishes the timescale of the topological fluctuations in the simulated cognitive map.

III. DISCUSSION

The topological model of the hippocampal cognitive map offers a connection between the spatial information processed by the individual place cells and the resulting global map emerging at the neuronal ensemble level, for both stable [24–29, 32] and transient [42–44] cell assembly networks. The elements of the model are embedded into the framework of simplicial topology: the groups of coactive cells are represented by abstract coactivity simplexes, whereas the spatial map encoded by the activity of neuronal populations is represented by the corresponding simplicial complexes. In particular, the formation and the disbanding of the cell groups is represented by the appearing and the disappearing coactivity simplexes, which combine into flickering coactivity complexes with nontrivial topological dynamics.

Generically, these dynamics occur at three principal timescales. The fastest timescale corresponds to the rapid recycling of the local connections—the starting point of the model. The large-scale topological loops, described by the time-dependent Betti numbers, unfold at a timescale that is by about an order of magnitude slower than the fluctuations at the simplex-level. Lastly, the topological fluctuations occur over certain robust base values that provide lasting, qualitative information about the environment.

The model demonstrates that, for sufficiently slow simplex-recycling rates, the topological fluctuations at the intermediate timescale freeze out, i.e., the simulated cognitive map may transition into a topologically stable state, with static (or nearly static) Betti numbers. Physiologically, this implies that if the hippocampal place cell assemblies rewire sufficiently slowly, then the hippocampal map may remain stable despite the recycling of the connections in its neuronal substrate. Thus, the model suggests that plasticity of neuronal connections, which is ultimately responsible for the network’s ability to incorporate new information [66–68], does not necessarily degrade the large-scale, qualitative information acquired by the system. Quite the opposite: renewing the connections allows correcting errors, e.g., removing some spurious, accidental topological obstructions fortuitously incorporated into the cognitive map. In other words, a network capable of not only accumulating, but also disposing information, exhibits better learning capacity, suggesting that physiological learning should involve a balanced contribution of both “learning” and “forgetting” components [69–71].

Remarkably, the three dynamic timescales suggested by the model have their direct biological counterparts: the *short-term memory*, which refers to temporary maintenance of ongoing (working) associations [72, 73], the *intermediate-term memory* that is acquired and updated at the “operational” timescale [74, 75], and the *long-term memory* that captures more persistent, qualitative

information are broadly recognized in the literature. Physiologically, these types of memory are associated with different parts of the brain (hippocampal and cortical networks); thus, the model reaffirms functional importance of the complementary learning systems for processing spatial information at different levels of spatiotemporal granularity, from a theoretical viewpoint [76–78].

The model allows exploring the effects produced on the cognitive map by the parameters of neuronal activity and the synaptic structure. For example, it can be shown, e.g., that the deterioration caused by an overly rapid decay of the network’s connections may be compensated by increasing neuronal activity, e.g., boosting the place cell firing rates [44] or via contributions of the “off-line,” endogenous activity of the hippocampal network—the so-called “place cell replays” [79, 80]. The latter are commonly viewed as manifestations of the animal’s “mental explorations” of its cognitive map [81–84] and are believed to help learning and to reinforce the map’s stability [85, 86]. This belief is largely validated by the model, which shows that sufficiently frequent, broadly distributed place cell replays, produced without temporal clustering, significantly reduce the topological fluctuations in the cognitive map C , thus helping to separate the fast and the slow timescales and to extract stable topological information for the long-term, qualitative representation of the environment [45]. Physiologically, these results suggest that indiscriminate, repetitive reactivations of memory sequences prevent deterioration of cognitive frameworks.

Dynamical simplicial complexes have previously appeared in physical literature as discrete models of quantum space-time fluctuations, in the context of Simplicial Quantum Gravity theories [87, 88]. It was shown that such complexes exhibit rich geometrical and topological dynamics, e.g., they can exist in different geometric phases, experience phase transitions between ordered and disordered states, etc., yielding regular behavior in the thermodynamic “classical” limit. Here dynamical complexes appear in a different context—as schematic models of the cognitive map’s topological structure [12, 89], which is naturally discrete (being encoded by finite neuronal populations) and transient due to the plasticity of the underlying network. Nevertheless, the statistical mechanics of these “neuronal” complexes also points at a variety of geometric and topological states developing at several timescales. In particular, using the instantaneous Betti numbers as intensive (size independent) statistical variables allows describing these complexes’ temporal architecture and identifying the emergent topological stability phenomena.

-
- [1] Leathers, M. & Olson, C. In Monkeys Making Value-Based Decisions, LIP Neurons Encode Cue Salience and Not Action Value, *Science* **338**: 132-135 (2012).
 - [2] Nitz, D. Tracking route progression in the posterior parietal cortex. *Neuron* **49**(5): 747-56 (2006).
 - [3] Muller, R., Ranck, J., Jr. & Taube J. Head direction cells: properties and functional significance. *Current Opinions Neurobiol.* **6**: 196-206 (1996).
 - [4] Taube, J. Head direction cells and the neurophysiological basis for a sense of direction. *Prog. Neurobiol.* **55**: 225-256 (1998).
 - [5] Terrazas, A., Krause, M., Lipa, P., Gothard, K., Barnes, C. & McNaughton, B. Self-motion and the hippocampal spatial metric. *J. Neurosci.* **25**: 8085-8096 (2005).
 - [6] Moser E. & Moser M-B. A metric for space. *Hippocampus* **18**: 1142-1156 (2008).
 - [7] Kropff, E., Carmichael, J., Moser, M.-B. & Moser E. Speed cells in the medial entorhinal cortex, *Nature* **523**: 419-424 (2015).
 - [8] Nitz, D. Spaces within spaces: rat parietal cortex neurons register position across three reference frames. *Nat. Neurosci.* **15**: 1365-1367 (2012).
 - [9] F. Sargolini, M. Fyhn, T. Hafting, B. McNaughton, M. Witter, M. Moser and E. Moser, Conjunctive Representation of Position, Direction, and Velocity in Entorhinal Cortex, *Science* **312**: 758-762 (2006).
 - [10] O'Keefe J. & Nadel, L. *The hippocampus as a cognitive map*. Oxford University Press (1978).
 - [11] Best, P., White A. & Minai, A. Spatial processing in the brain: the activity of hippocampal place cells. *Ann. Rev. Neurosci.* **24**: 459-486 (2001).
 - [12] Babichev, A., Cheng, S. & Dabaghian, Y. Topological schemas of cognitive maps and spatial learning. *Front. Comput. Neurosci.* **10**:18 (2016).
 - [13] O'Keefe, J. & Dostrovsky, J. The hippocampus as a spatial map. Preliminary evidence from unit activity in the freely-moving rat. *Brain Res.* **34**(1): 171-5 (1971).
 - [14] Gothard, K., Skaggs, W. & McNaughton, B. Dynamics of mismatch correction in the hippocampal ensemble code for space: interaction between path integration and environmental cues, *J Neurosci.* **16**: 8027-8040 (1996).
 - [15] Leutgeb, J., Leutgeb, S., Treves, A., Meyer, R., Barnes, C. et al. Progressive transformation of hippocampal neuronal representations in "morphed" environments. *Neuron* **48**: 345-358 (2005).
 - [16] Wills, T., Lever, C., Cacucci, F., Burgess, N. & O'Keefe, J. Attractor dynamics in the hippocampal representation of the local environment. *Science* **308**: 873-876 (2005).
 - [17] Touretzky, D., Weisman, W., Fuhs, M., Skaggs, W., Fenton, A. et al. Deforming the hippocampal map. *Hippocampus* **15**: 41-55 (2005).
 - [18] Poucet, B. & Herrmann, T. Exploratory patterns of rats on a complex maze provide evidence for topological coding. *Behav Processes* **53**: 155-162 (2001).
 - [19] Diba, K. & Buzsaki, G. Hippocampal network dynamics constrain the time lag between pyramidal cells across modified environments. *J Neurosci.* **28**: 13448-13456 (2008).
 - [20] Alvernhe, A., Sargolini, F. & Poucet, B. Rats build and update topological representations through exploration. *Anim. Cogn.* **15**: 359-368 (2012).
 - [21] Wu, X. & Foster, D. Hippocampal replay captures the unique topological structure of a novel environment. *J Neurosci.* **34**: 6459-6469 (2014).
 - [22] Chen, Z., Gomperts, S.N., Yamamoto, J. & Wilson, M.A. Neural representation of spatial topology in the rodent hippocampus. *Neural computation* **26**: 1-39 (2014).

- [23] Dabaghian, Y., Brandt, V. & Frank, L. Reconceiving the hippocampal map as a topological template. *eLife* 10.7554/eLife.03476: 1-17 (2014).
- [24] Dabaghian, Y., Mémoli, F., Frank, L. & Carlsson, G. A Topological Paradigm for Hippocampal Spatial Map Formation Using Persistent Homology. *PLoS Comput. Biol.* **8**: e1002581 (2012).
- [25] Arai, M., Brandt, V. & Dabaghian, Y. The effects of theta precession on spatial learning and simplicial complex dynamics in a topological model of the hippocampal spatial map. *PLoS Comput. Biol.* **10**: e1003651 (2014).
- [26] Basso, E., Arai, M. & Dabaghian, Y. The effects of gamma synchronization on spatial learning in a topological model of the hippocampal spatial map, *PloS Comput. Biol.* **12**:9 (2016).
- [27] Hoffman, K., Babichev, A. & Dabaghian, Y. A model of topological mapping of space in bat hippocampus. *Hippocampus*, **26**: 13451353 (2016).
- [28] Dabaghian, Y. Through synapses to spatial memory maps: a topological model. *Sci. Reports* **9**: 572 (2018).
- [29] Dabaghian, Y. From topological analyses to functional modeling: the case of hippocampus. In submission, (2019).
- [30] Buzsaki, G. Neural syntax: cell assemblies, synapsembles, and readers. *Neuron* **68**: 362-385 (2010).
- [31] Harris, K., Csicsvari, J., Hirase, H., Dragoi, G. & Buzsaki, G. Organization of cell assemblies in the hippocampus. *Nature* **424**: 552-556 (2003).
- [32] Babichev, A., Mémoli, F., Ji, D. & Dabaghian, Y. A topological model of the hippocampal cell assembly network. *Frontiers in Comput. Neurosci.* **10**:50 (2016).
- [33] Billeh, Y., Schaub, M., Anastassiou, C., Barahona, M. & Koch C. Revealing cell assemblies at multiple levels of granularity. *J. Neurosci. Methods* **236**: 92-106 (2014).
- [34] Goldman-Rakic, P. Cellular basis of working memory. *Neuron* **14**: 477-485 (1995).
- [35] Hiratani, N. & Fukai, T. Interplay between Short- and Long-Term Plasticity in Cell-Assembly Formation. *PLoS One* **9**: e101535 (2014).
- [36] Whittington, M., Traub, R., Kopell, N., Ermentrout, B. & Buhl, E. Inhibition-based rhythms: experimental and mathematical observations on network dynamics. *Int J Psychophysiol.* **38**: 315-336 (2000).
- [37] Bi, G. & Poo, M. Synaptic modification by correlated activity: Hebb's postulate revisited. *Annu. Rev. Neurosci.* **24**: 139-166 (2001).
- [38] Bennett, S., Kirby, A. & Finnerty, G. Rewiring the connectome: Evidence and effects. *Neurosci. Biobehav. Rev.* **88**: 5162 (2018).
- [39] Meck, W., Church, R. & Olton, D. Hippocampus, time, and memory. *Behav. Neurosci.* **127**: 655-668 (2013).
- [40] Clayton, N., Bussey, T. & Dickinson, A. Can animals recall the past and plan for the future? *Nat. Rev. Neurosci.* **4**: 685-691 (2003).
- [41] Brown, M., Farley, R. & Lorek, E. Remembrance of places you passed: Social spatial working memory in rats. *J. Exper. Psych.: Animal Behav. Processes* **33**: 213-224 (2007).
- [42] Babichev, A. & Dabaghian, Y. Persistent Memories in Transient Networks. *Springer Proc. Phys.* **191**: 179-188 (2017).
- [43] Babichev, A. & Dabaghian, Y. Transient cell assembly networks encode stable spatial memories. *Sci. Rep.* **7**: 3959 (2017).
- [44] Babichev, A., Morozov, D. & Dabaghian, Y. Robust spatial memory maps encoded by networks with transient connections. *PLoS Comput. Bio.* **14**(9): e1006433 (2018).
- [45] Babichev, A., Morozov, D. & Dabaghian, Y. Replays of spatial memories suppress topological fluctuations in cognitive map. *Network Neuroscience*, Special Issue: Topological Neuroscience, **3**(3):

- 707-724 (2019).
- [46] Hatcher, A. *Algebraic topology*. Cambridge University Press (2002).
 - [47] Aleksandrov, P. *Elementary concepts of topology*, New York: F. Ungar Pub. Co. (1965).
 - [48] Ghrist, R. Barcodes: The persistent topology of data. *Bull. Amer. Math. Soc.* **45**: 61-75 (2008).
 - [49] Singh, G., Mémoli, F., Ishkhanov, T., Sapiro, G., Carlsson, G & Ringach D. Topological analysis of population activity in visual cortex. *J. Vis.* **8**(11): 1-18 (2008).
 - [50] Carlsson, G. Topology and data. *Bull. Amer. Math. Soc.* **46**: 255-308 (2009).
 - [51] Lum, P., Singh, G., Lehman, A., Ishkanov, T., Vejdemo-Johansson, M., Alagappan, M., Carlsson, J. & Carlsson, G. Extracting insights from the shape of complex data using topology. *Sci. Rep.* **3**: 1236 (2013).
 - [52] Zomorodian, A. & Carlsson, G. Computing persistent homology. *Dis. & Comput. Geometry* **33**: 249–274 (2005).
 - [53] Carlsson, G. & Silva, Vd. Zigzag Persistence. *Found. Comput. Math.* **10**: 367-405 (2010).
 - [54] Carlsson, G., Silva, Vd. & Morozov, D. Zigzag persistent homology and real-valued functions. *Proceedings of the 25th annual symposium on Computational geometry*. Aarhus, Denmark: ACM. pp. 247-256 (2009).
 - [55] Edelsbrunner, H., Letscher, D. & Zomorodian, A. Topological Persistence and Simplification. *Discrete & Computational Geometry* **28**: 511–533 (2002).
 - [56] Zomorodian, A., *Topology for computing*, Cambridge University Press (2005).
 - [57] Edelsbrunner, H. & Harer, J. *Computational topology: an introduction*. Amer. Math. Soc. (2010).
 - [58] Burgess, N. & O’Keefe, J. Cognitive graphs, resistive grids, and the hippocampal representation of space. *J Gen. Physiol.* **107**: 659-662 (1996).
 - [59] Muller, R., Stead, M. & Pach, J. The hippocampus as a cognitive graph. *J Gen. Physiol.* **107**: 663-694 (1996).
 - [60] Jonsson, J. *Simplicial complexes of graphs*. Springer (2008).
 - [61] Mizuseki, K., Sirota, A., Pastalkova, E. & Buzsaki, G. Theta oscillations provide temporal windows for local circuit computation in the entorhinal-hippocampal loop. *Neuron* **64**: 267-280 (2009).
 - [62] Thompson, L. & Best, P. Long-term stability of the place-field activity of single units recorded from the dorsal hippocampus of freely behaving rats. *Brain. Res.* **509**: 299-308 (1990).
 - [63] Shapiro M. Plasticity, hippocampal place cells, and cognitive maps. *Arch. Neurol.* **58**: 874-881 (2001).
 - [64] Fenton, A. A. & R. U. Muller. Place cell discharge is extremely variable during individual passes of the rat through the firing field. *Proc. Natl. Acad. Sci.* **95**(6): 3182-3187 (1998).
 - [65] Gromov, M. On the number of simplexes of subdivisions of finite complexes. *Mathematical notes of the Acad.Sci. USSR* **3**: 326-332 (1968).
 - [66] McHugh, T. & Tonegawa, S. CA3 NMDA receptors are required for the rapid formation of a salient contextual representation. *Hippocampus* **19**: 1153-1158 (2009).
 - [67] Leuner, B. & Gould, E. Structural plasticity and hippocampal function. *Annu. Rev. Psychol.* **61**: 111-140 (2010).
 - [68] Schaefer, A., Grafen, K., Teuchert-Noodt, G. & Winter, Y. Synaptic remodeling in the dentate gyrus, CA3, CA1, subiculum, and entorhinal cortex of mice: effects of deprived rearing and voluntary running. *Neural Plast.* **2010**:11 (2010).
 - [69] Dupret, D., Fabre, A., Döbrössi, M., Panatier, A., Rodriguez, J. Lamarque, S., Lemaire, V., Olier, S., Piazza, P. & Abrous, D. Spatial learning depends on both the addition and removal of new hippocampal neurons. *PLoS Biol.* **5**:e214 (2007).
 - [70] Kuhl, B., Shah, A., DuBrow, S. & Wagner, A. Resistance to forgetting associated with hippocampus-mediated reactivation during new learning. *Nat. Neurosci.* **13**: 501-506 (2010).

- [71] Murre, J., Chessa, A. & Meeter, M. A mathematical model of forgetting and amnesia. *Frontiers in Psych.* **4**:76 (2013).
- [72] Cowan, N. What are the differences between long-term, short-term, and working memory? *Prog. Brain Res.* **169**: 323-338 (2008).
- [73] Hebb, D. *The organization of behavior; a neuropsychological theory*. Wiley (1949).
- [74] Eichenbaum, H., Otto, T. & Cohen, N. Two functional components of the hippocampal memory system. *Behavioral and Brain Sciences* **17**: 449-472 (1994).
- [75] Kesner, R. & Hunsaker, M. The temporal attributes of episodic memory. *Behav. Brain Res.* **215**: 299-309 (2010).
- [76] McClelland, J., McNaughton, B. & O'Reilly R. Why there are complementary learning systems in the hippocampus and neocortex: insights from the successes and failures of connectionist models of learning and memory. *Psychol Rev.* **102**: 419-457 (1995).
- [77] Fusi, S., Drew, P. & Abbott, L. Cascade Models of Synaptically Stored Memories. *Neuron* **45**: 599-611 (2005).
- [78] O'Reilly, R. & McClelland, J. Hippocampal conjunctive encoding, storage, and recall: Avoiding a trade-off. *Hippocampus* **4**: 661-682 (1994).
- [79] Karlsson, M. & Frank L. Awake replay of remote experiences in the hippocampus. *Nat. Neurosci.* **12**: 913-918 (2009).
- [80] Dragoi, G. & Tonegawa, S. Preplay of future place cell sequences by hippocampal cellular assemblies. *Nature* **469**: 397-401 (2011).
- [81] Foster, D. & Wilson, M. Reverse replay of behavioural sequences in hippocampal place cells during the awake state. *Nature* **440**: 680-683 (2006).
- [82] Johnson. A. & Redish, A. Neural Ensembles in CA3 Transiently Encode Paths Forward of the Animal at a Decision Point. *J. Neurosci.* **27**: 12176-12189 (2007).
- [83] Hopfield, J. Neurodynamics of mental exploration. *Proc. Natl. Acad. Sci.* **107**: 1648-1653 (2010).
- [84] Dabaghian, Y. Maintaining Consistency of Spatial Information in the Hippocampal Network: A Combinatorial Geometry Model. *Neural Comput.* **28**: 1051-1071 (2016).
- [85] Roux, L., Hu, B., Eichler, R., Stark, E. & Buzsaki, G. Sharp wave ripples during learning stabilize the hippocampal spatial map. *Nat. Neurosci.* **20**:845-853 (2017).
- [86] Girardeau, G., Benchenane, K., Wiener, S., Buzsaki, G. & Zugaro, M. Selective suppression of hippocampal ripples impairs spatial memory. *Nat. Neurosci.* **12**: 1222-1223 (2010).
- [87] Ambjørn, J., Carfora, M. & Marzuoli, A. *The geometry of dynamical triangulations*, Springer. Berlin; New York, (1997).
- [88] Hamber, H. *Quantum gravitation: the Feynman path integral approach*, Berlin: Springer (2009).
- [89] Babichev, A. & Dabaghian, Y. Topological schemas of memory spaces. *Frontiers Comput. Neurosci.* **12**, 10.3389/fncom.2018.00027 (2018).